Activation and Inhibition of Skeletal RyR Channels by a Part of the Skeletal DHPR II-III Loop: Effects of DHPR Ser^{687} and FKBP12

Angela F. Dulhunty, Derek R. Laver, Esther M. Gallant, Marco G. Casarotto, Suzy M. Pace, and Suzanne Curtis
Muscle Research Group, John Curtin School of Medical Research, Canberra, ACT 2601, Australia

ABSTRACT Peptides, corresponding to sequences in the N-terminal region of the skeletal muscle dihydropyridine receptor (DHPR) II-III loop, have been tested on sarcoplasmic reticulum (SR) Ca^{2+} release and ryanodine receptor (RyR) activity. The peptides were: A1, Thr^{671}-Leu^{690}; A2, Thr^{671}-Leu^{690} with Ser^{687} Ala substitution; NB, Gly^{689}-Lys^{708} and A1S, scrambled A1 sequence. The relative rates of peptide-induced Ca^{2+} release from normal (FKBP12+) SR were A2 > A1 > A1S > NB. Removal of FKBP12 reduced the rate of A1-induced Ca^{2+} release by ~30%. A1 and A2 (but not NB or A1S), in the cytoplasmic (*cis*) solution, either activated or inhibited single FKBP12+ RyRs. Maximum activation was seen at −40 mV, with 10 μM A1 or 50 nM A2. The greatest A1-induced increase in mean current (sixfold) was seen with 100 nM *cis* Ca^{2+}. Inhibition by A1 was greatest at +40 mV (or when permeant ions flowed from cytoplasm to SR lumen) with 100 μM *cis* Ca^{2+}, where channel activity was almost fully inhibited. A1 did not activate FKBP12-stripped RyRs, although peptide-induced inhibition remained. The results show that peptide A activation of RyRs does not require DHPR Ser^{687}, but required FKBP12 binding to RyRs. Peptide A must interact with different sites to activate or inhibit RyRs, because current direction-, voltage-, *cis* [Ca^{2+}]-, and FKBP12-dependence of activation and inhibition differ.

INTRODUCTION

The ryanodine receptor (RyR) calcium channel mediates Ca^{2+} release from internal stores in many cell types and is an essential component of excitation-contraction coupling (ECC) in striated muscle. In skeletal muscle, the L-type Ca^{2+} channel (dihydropyridine receptor, DHPR) is the voltage sensor for ECC, i.e., it senses T-tubule depolarization and transmits a signal to the RyR, via a protein-protein interaction which requires the loop between the second and third repeats of the skeletal DHPR α_1 subunit (II-III loop; Tanabe et al., 1990). The II-III loop of the DHPR binds to a 37-amino acid sequence, Arg^{1076}-Asp^{1112}, in the skeletal muscle RyR (Leong and Maclennan, 1998).

The skeletal DHPR II-III loop increases [^{3}H]ryanodine binding to sarcoplasmic reticulum (SR) vesicles, and activates purified RyR channels in lipid bilayers (Lu et al., 1994, 1995). Because ryanodine binds preferentially to open RyR channels, the increase in [^{3}H]ryanodine binding suggests that native RyRs in SR vesicles are activated by the II-III loop. The N-terminal part of the II-III loop (Glu^{666}-Glu^{726}) also activates RyR channels, but fails to do so when Ser^{687} is either phosphorylated or replaced by alanine (Lu et al., 1995). A short peptide Thr^{671}-Leu^{690} (peptide A) activates Ca^{2+} release from SR, but peptides corresponding to other segments of the loop do not (El-Hayek et al., 1995; El-Hayek and Ikemoto, 1998). Since the actions of peptide A on single RyR channels had not been reported, we examined its effects on RyRs. We also studied possible interactions between the regulation of RyRs by peptide A and their regulation by the FK506-binding protein (FKBP12), a co-protein that coordinates RyR activity. FKBP12 is intrinsic to normal RyR function and may be involved in ECC (Ahern et al., 1994, 1997a; Brillantes et al., 1994; Mayrleitner et al., 1994; Lamb and Stephenson, 1996). Four FK506-binding proteins (FKBP12, M_r ~12,000) are tightly bound to each RyR monomer (Jayaraman et al., 1992; Timerman et al., 1993; Wagenknecht et al., 1996, 1997). The immunosuppressant drugs FK506 and rapamycin bind to FKBP12 and dissociate it from the RyR (Timerman et al., 1993, 1995). RyRs "stripped" of their FKBP12 co-proteins display increased channel activity at low cytoplasmic Ca^{2+} concentrations, with a loss of coordinated channel opening to the maximum conductance (Ahern et al., 1997a).

In this study, the ability of peptide A1 (Thr^{671}-Leu^{690}) and peptide A2 (with Ser^{687} replaced by Ala^{687}) to release Ca^{2+} from native FKBP12+ terminal cisternae (TC) vesicles and from FKBP12-stripped vesicles was examined, as well as the actions of the peptides on single native RyR channels incorporated into lipid bilayers. The results showed that peptide A1 released Ca^{2+} from FKBP12+ and FKBP12-stripped TC vesicles, although release from the RyRs lacking FKBP12 was markedly reduced. Ca^{2+} release by peptide A2 was greater than that by peptide A1. The peptides had a dual action on RyR channel activity. Activation at −40 mV was greatest with 100 nM *cis* Ca^{2+}, while inhibition at +40 mV was strongest with 100 μM *cis* Ca^{2+}. Channel activation by the peptide was markedly reduced in FKBP12-stripped RyRs. The inhibition of channel activity was strongest when current flowed from the cytoplasmic to the luminal side of the RyR and preferentially blocked channel opening to maximum conductance levels. The re-

Received for publication 22 July 1998 and in final form 5 April 1999.

Address reprint requests to Dr. A. F. Dulhunty, John Curtin School of Medical Research, Australian National University, P.O. Box 334, Canberra, ACT 2601, Australia. Tel.: 61 6 249 4491; Fax: 61 6 249 4761; E-mail: angela.dulhunty@anu.edu.au.

0006-3495/99/07/189/15 $2.00

sults show that these small DHPR II-III loop peptides can both activate and inhibit single RyR channels and are likely to act on at least two separate sites on the RyR channel protein.

METHODS

Materials

Rapamycin was obtained from Calbiochem and as a gift from Wyeth-Ayerst (Princeton, NJ). Other chemicals and biochemicals were from Sigma-Aldrich (Castle Hill, Australia). The DHPR II-III loop peptides were synthesized using an Applied Biosystems 430A Peptide Synthesiser with purification to 98 to 100% using HPLC and mass spectroscopy. Peptide conformation was determined using NMR. Stock peptide solutions (~2 mM) were prepared in H_20 and frozen in 20-μl aliquots. Precise stock solution concentrations were determined (Auspep Pty Ltd) using acid hydrolysis followed by a standardized PTC (phenylthiocarbamyl) protocol and analyzed by reverse phase HPLC. The following peptides were used in this study.

Peptide A1

^{671}Thr Ser Ala Gln Lys Ala Lys Ala Glu Glu Arg Lys Arg Arg Lys Met Ser Arg Gly Leu^{690}.

Peptide A2

^{671}Thr Ser Ala Gln Lys Ala Lys Ala Glu Glu Arg Lys Arg Arg Lys Met Ala Arg Gly Leu^{690}.

Peptide NB

^{689}Gly Leu Pro Asp Lys Thr Glu Glu Glu Lys Ser Val Met Ala Lys Lys Leu Glu Gln Lys^{708}.

Peptide A1S

Thr Arg Lys Ser Arg Leu Ala Arg Gly Gln Lys Ala Lys Ala Lys Ser Glu Met Arg Glu.

Vesicle preparation

SR vesicles were isolated from the back and leg muscles of New Zealand White rabbits using methods described by Saito et al. (1984) with minor modifications (Ahern et al., 1994, 1997a). Native FKBP12+ TC vesicles were obtained from the 38%/45% sucrose interface after sucrose gradient centrifugation. FKBP12 was "stripped" from TC vesicles by incubating the vesicles with 20 μM rapamycin for 20 min at 37°C, followed by centrifugation at 540,000 $\times$ *g* (and then resuspension) to remove rapamycin and the FKBP12-rapamycin complex. The amount of FKBP12 remaining bound to the TC vesicles was assessed by immunostaining Western blots of the vesicles with anti-peptide antibodies raised against peptides corresponding to the N-terminal sequence of FKBP12. The incubation procedure with rapamycin removed all detectable FKBP12 from each of the 14 preparations used in the present experiments. "FKBP12+-incubated" vesicles, incubated for 20 min at 37°C in the absence of rapamycin, retained an amount of FKBP12 similar to that seen in native B4 vesicles. Details of the FKBP12 "stripping" procedure, production of anti-peptide antibodies, electrophoresis, and Western blotting are given in Ahern et al. (1997a).

Calcium release from TC vesicles

Extravesicular Ca^{2+} was monitored at 710 nm with the Ca^{2+} indicator, antipyrylazo III, using a Cary 3 spectrophotometer. Identical release experiments, performed at 790 nm, showed no changes in optical density (OD) that would alter the rate of Ca^{2+} uptake measured from recordings at 710 nm. A step increase in OD upon addition of ruthenium red was seen in recordings at both 710 nm and 790 nm, and was subtracted from the records shown in Figs. 1 and 2 (see Results). The temperature of the cuvette solution was thermostatically controlled at 25°C and the solution was stirred with a magnetic stirrer. Ca^{2+} release was measured as described by Timerman et al. (1993). TC vesicles (100 μg protein) were added to the cuvette, to a final volume of 2 ml, of a solution containing (in mM): 100, KH_2PO_4 (pH = 7); 4, $MgCl_2$; 1, Na_2ATP; 0.5, antipyrylazo III). Vesicles were partially loaded with Ca^{2+} by four sequential additions of $CaCl_2$, each initially increasing the extravesicular [Ca^{2+}] by ~7.5 μM (see Figs. 1 and 2). It was necessary to also suppress Ca^{2+},Mg^{2+}-ATPase activity after loading (using thapsigargin, 200 nm; Sagara and Inesi, 1991), to allow extravesicular [Ca^{2+}] to increase after activation of the RyR. Peptide or caffeine were the then added, followed by the RyR blocker ruthenium red (to a final concentration of 5 μM), to determine whether Ca^{2+} release through RyR channels was responsible for Ca^{2+} release from SR. The Ca^{2+} ionophore A23187 (3 μg/ml) was finally added to release the Ca^{2+} remaining in the TC vesicles. A calibration curve was established at the start of each experiment by measuring OD changes in response to four sequential additions of 12.5 μM $CaCl_2$.

Lipid bilayers

Experiments were carried out at 20–25°C. The techniques are described in Ahern et al. (1994) and Laver et al. (1995). Bilayers were formed from phosphatidylethanolamine, phosphatidylserine, and phosphatidylcholine (5:3:2 w/w) (Avanti Polar Lipids, Alabaster, AL) across an aperture with a diameter of 200–250 μm in the wall of a 1.0-ml Delrin cup (Cadillac Plastics, Australia). In some experiments (e.g., Fig. 7) bilayers contained only phosphatidylethanolamine and phosphatidylcholine (8:2 w/w). In these experiments the negatively charged phosphatidylserine was left out to remove possible effects on channel activity of bilayer surface potential changes during changes in ionic composition.

TC vesicles (final concentration, 10 μg/ml) and drugs were added to the *cis* chamber. The bilayer potential was controlled, and single channel activity recorded, using an Axopatch 200A amplifier (Axon Instruments, Foster City, CA). For experimental purposes, the *cis* chamber was held at ground and the voltage of the *trans* chamber controlled. Bilayer potential is expressed in the conventional way as $V_{cis} - V_{trans}$, (i.e., $V_{cytoplasm} - V_{lumen}$).

Bilayer solutions

Bilayers were formed and vesicles incorporated into the bilayer using a *cis* solution containing 250 mM CsCl (or 230 mM cesium methanesulfonate (MS) plus 20 mM CsCl), 1 mM $CaCl_2$, and 10 mM *N*-tris[hyroxymethyl] methyl-2-aminoethanesulfonic acid (TES, pH 7.4 with CsOH) and a *trans* solution containing 50 mM CsCl (or 30 mM CsMS plus 20 mM CsCl), 1 mM $CaCl_2$, and 10 mM TES (pH 7.4). To prevent incorporation of multiple channels into the bilayer, the *cis* solution was replaced by perfusion of the *cis* chamber as soon as channel activity was observed. The *cis* perfusion solution was identical to the initial *cis* solution, except that the [Ca^{2+}] was varied (10^{-7} M or 10^{-4} M) as required. Ca^{2+} was buffered to 10^{-7} M or 10^{-5} M using 1 mM BAPTA; 200 mM CsMS was added to the *trans* chamber after channel incorporation to give symmetrical solutions.

In experiments examining RyR channel activity over a range of peptide concentrations and at +40 mV and −40 mV, bilayer potential was changed every 30 s over a 2-min period after each addition of drugs or peptides to the *cis* chamber. Control activity was recorded for 2 min after addition of 200 mM CsMS to the *trans* chamber. Activity was then recorded for 2 min after *cis* additions of 2 mM Na_2ATP, 4 mM $MgCl_2$, or 2 mM $MgCl_2$ and

then after each aliquot of peptide (three to eight different peptide concentrations were examined in each channel). Peptides were perfused out of the *cis* chamber, and the channels were reexposed to Na_2ATP plus $MgCl_2$ and then finally to ruthenium red (10–80 μM). In some experiments 5 mM Ca^{2+} and 250 mM or 500 mM mannitol were added to the *cis* solution to aid vesicle incorporation.

Recording and analysis of single channel activity

Currents were filtered at 1 kHz (10-pole low-pass Bessel, −3 dB) and digitized at 5 kHz. Analysis of single channel records (using *Channel 2,* developed by P. W. Gage and M. Smith) yielded channel open probability (P_o), frequency of events (F_o), open times, closed times, and mean open or closed times (T_o or T_c) as well as mean current (I'). The event discriminator was set above the baseline noise at ~20% of the maximum current, rather than the usual 50%, so that openings to both subconductance and maximum conductance levels were included in the analysis. Channel activity was analyzed over two 30-s periods of continuous activity at +40 mV and two 30-s periods of continuous activity at −40 mV.

Values for the peptide concentration required for 50% activation (AC_{50}) and for 50% inhibition (IC_{50}) of mean current (I') were obtained from graphs of I' as a function of peptide concentration, [P] (Figs. 5 and 6). Some data were fitted with the equation

$$I' = (I'_c + I'_{max}/(1 + AC_{50}/[P]))/(1 + ([P]/IC_{50})^H)$$

where I'_c is the control I', I'_{max} is the maximum current during activation, and H is the Hill coefficient.

Statistics

Average data are given as mean ± SEM. The significance of the difference between control and test values was tested 1) using a Student's *t*-test, either one- or two-sided and either for independent or paired data, as appropriate; or 2) using the nonparametric "sign" test (Minium et al., 1993). Differences were considered to be significant when $p \leq 0.05$.

RESULTS

Peptide A1 releases Ca^{2+} from terminal cisternae

The ability of peptide A1 to release Ca^{2+} from native FKBP12+ TC vesicles was examined. As previously reported (El-Hayek et al., 1995; El-Hayek and Ikemoto, 1998), A1 released Ca^{2+} from TC. In the present experiments, extravesicular [Ca^{2+}] increased when 200 nM thapsigargin was added to the cuvette after loading the SR with Ca^{2+} (Fig. 1, *A* and *D*).

The rate of Ca^{2+} release with thapsigargan, just before adding the peptide, was ~55 nM/mg/min. Addition of peptide NB did not alter the rate of Ca^{2+} release, A1S induced a small increase in Ca^{2+} release, and A1 caused a larger increase (Fig. 1, *A–C*). Ruthenium red (10 μM) stopped Ca^{2+} release, if added while extravesicular [Ca^{2+}] was increasing (Fig. 1, *A* and *D*), suggesting that the Ca^{2+} release after addition of thapsigargin (Fig. 1 *D*), and activated by peptides A1 and A1S (Fig. 1 *A*), was through RyR channels. The rate of Ca^{2+} release induced by peptide A1 (maximum rate after A1 addition minus the rate in the presence of thapsigargin) of ±8 nmol/mg/min with 36 μM A1 ($n = 8$) was significantly greater ($p = 0.007$) than the 56 ± 10 nmol/mg/min with 36 μM A1S ($n = 6$, Fig. 1 *E*).

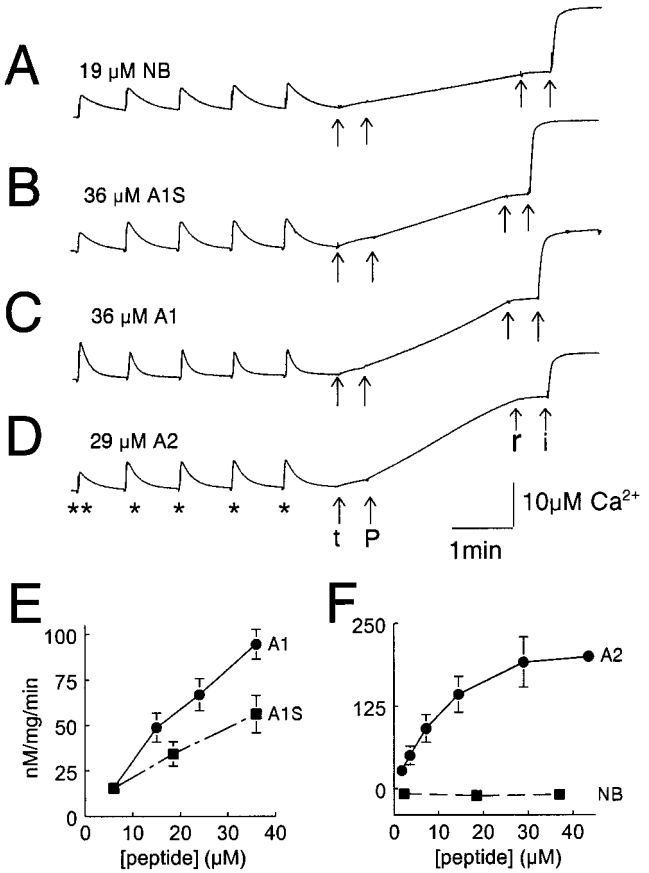

FIGURE 1 Peptides A1S, A1, and A2 release Ca^{2+} from partially loaded native FKBP12+ TC vesicles. (*A*)–(*D*) Records of OD changes at 710 nm, with changes in extravesicular [Ca^{2+}], measured using antipyrylazoIII (500 μM) as the Ca^{2+} indicator. In each record, extravesicular [Ca^{2+}] increased when TC vesicles were added to the cuvette (**) and then declined as Ca^{2+} was sequestered by the TC vesicles. The next four positive deflections (*) indicate addition of each aliquot of $CaCl_2$ (7.5 μM, final concentration). The first arrow (*t*) indicates addition of 200 nM thapsigargin to block the SR Ca^{2+} ATPase. The second arrow (*P*) indicates addition of (*A*) 19 μM NB; (*B*) 36 μM A1S; (*C*) 36 μM A1; (*D*) 29 μM A2. Ruthenium red (10 μM) was added at the third arrow (*r*), before the ionophore A23187 (*last arrow, i*, 3 μg/ml). The vertical calibration is in μM Ca^{2+} (addition of 10 μM extravesicular Ca^{2+}, increased OD by 0.2 units). (*E*) Maximum rate of Ca^{2+} release (nM/mg of TC vesicles/min) induced by peptides A1 ($n = 8$, *filled circles*) or A1S ($n = 6$; *filled squares*). (*F*) Maximum rate of Ca^{2+} release (nM/mg/min) induced by peptide A2 ($n = 11$; *filled circles*) or NB ($n = 3$; *filled squares*) as a function of peptide concentration. The rates shown are the maximum rate of release with peptide minus the preceding rate with thapsigargin. Data points are averages ± SE, using TC vesicles from three different SR preparations.

Activation by A1S suggests that peptides containing positively charged residues in any sequence can induce Ca^{2+} release from SR, via activation of RyRs. This observation is consistent with the ability of polylysine to release Ca^{2+} from SR (El-Hayek and Ikemoto, 1998).

Ser^{687} is not essential for peptide activation of Ca^{2+} release from SR

Surprisingly, and in contrast to results obtained with the full-length II-III loop peptide (Lu et al., 1995), the Ser^{687}

Ala substitution increased the ability of peptide A to activate Ca^{2+} release from native FKBP12+ TC vesicles. Ca^{2+} release induced by A2 was significantly ($p < 0.05$) greater than that induced by peptide A1 and increased to 191 ± 38 nM/mg/min ($n = 11$) with 29 μM peptide (*filled circles*, Fig. 1 *F*). As with A1, the A2-induced Ca^{2+} release from SR was substantially reduced by 10 μM ruthenium red (Fig. 1 *D*) and was thus through RyR channels.

Ca^{2+} release with A1 is less after FKBP12 removal

The experiments were repeated with FKBP12+-incubated and with FKBP12-stripped TC vesicles. FKBP12-stripped vesicles required longer loading times than native or FKBP+-incubated vesicles (12 of 12 preparations) as expected from the greater RyR activity after FKBP12 removal (Ahern et al., 1994, 1997a; Table 4). Since the rate of depletion of extravesicular Ca^{2+} is equal to the rate of Ca^{2+} uptake minus the rate of Ca^{2+} release, load time increases if release increases. The time allowed for loading was increased to ~4 min between each addition of $CaCl_2$ for both FKBP12+-incubated and FKBP12-stripped TC (prepared in parallel from the same native TC preparation). Data were obtained from vesicles from at least three different preparations. The amount of Ca^{2+} loaded, determined from the difference between the OD after the last load step and the OD 4 min after A23187 addition, was 94.0 ± 0.3% ($n = 25$) of the Ca^{2+} added to the extravesicular solution for FKBP12+-incubated and 93.1 ± 0.7% ($n = 22$) in FKBP12-stripped vesicles. Peptide A1 (36 μM) was significantly less effective at releasing Ca^{2+} from FKBP12-stripped TC (Fig. 2 *B*) than from the FKBP12+-incubated TC (Fig. 2 *A*) at all peptide concentrations (Fig. 2 *C*).

The reduced Ca^{2+} release from FKBP12-stripped vesicles might have been due to factors other than the absence of FKBP12. For example, the number of vesicles containing active RyR channels might have been reduced after FKBP12 removal. To test this possibility, the amount of Ca^{2+} that could be released through RyR channels ("releasable Ca^{2+}") was measured by adding 5 mM caffeine after thapsigargin, and expressing the increase in extravesicular [Ca^{2+}] after 6 min as a fraction of the Ca^{2+} loaded. Releasable Ca^{2+} was 64 ± 10 5% in FKBP12+-incubated TC and 54 ± 4% in the FKBP12-stripped TC (each number is the average from two different preparations). The effect of FKBP12 removal on the ability of the TC to release Ca^{2+} in general was examined by looking at the release in response to 0.5 mM caffeine (a submaximal concentration). The maximum rate of Ca^{2+} release in response to caffeine was expressed as a fraction of the releasable Ca^{2+}. The rates were 13 ± 3%/min ($n = 2$) for FKBP12+-incubated TC and 12 ± 1%/min ($n = 2$) for FKBP12-stripped TC. Thus the rates of release in response to caffeine were not influenced by FKBP12 removal.

Rates of A1-activated Ca^{2+} release were adjusted for differences in the amounts of releasable Ca^{2+} between

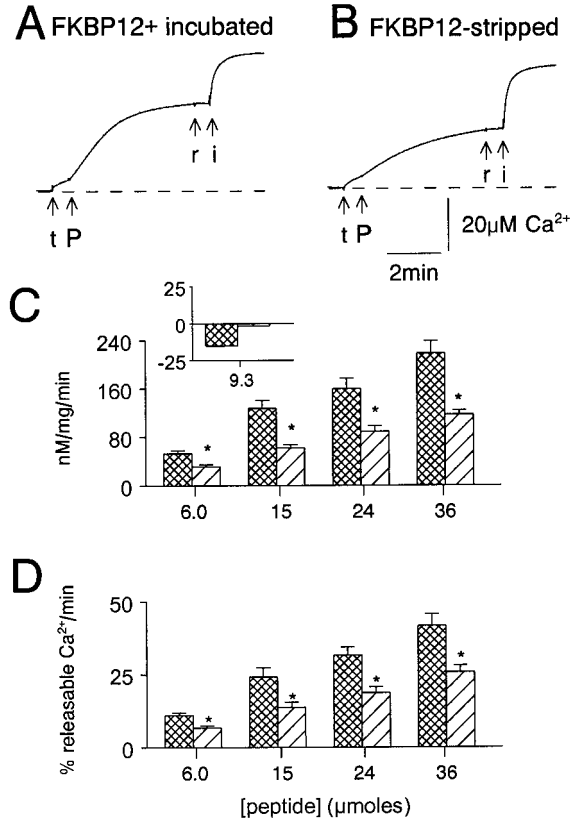

FIGURE 2 Peptide A1-induced Ca^{2+} release from partially loaded FKBP12-stripped TC vesicles was less than that from FKBP12+-incubated TC. (*A*) and (*B*) show records of OD changes at 710 nm, with changes in extravesicular [Ca^{2+}], using antipyrylazoIII (500 μM) as a Ca^{2+} indicator. The Ca^{2+} loading procedure is the same as in Fig. 1. The first arrow (*t*) in each record indicates the addition of 200 nM thapsigargin. The second arrow (*P*) indicates addition of 36 μM of peptide A1 to (*A*) FKBP12+-incubated vesicles and (*B*) FKBP12-stripped vesicles. Ruthenium red (*third arrow, r*, 10 μM) was added before the ionophore A23187 (*last arrow, i*, 3 μg/ml). The vertical calibration is in μM of Ca^{2+} (adding 10 μM extravesicular Ca^{2+} increased OD by 0.2 units). (*C*) Histograms of the initial rate of Ca^{2+} release (nM/mg/min of TC vesicle) in the presence of peptide A1 (6–36 μM), from FKBP12+-incubated ($n = 6$; *double cross-hatched bars*) or FKBP12-stripped ($n = 6$; *cross-hatched bars*). Rates are the maximum rate with peptide minus the preceding rate with thapsigargin. (*C, inset*) Rate of Ca^{2+} release after adding peptide NB minus the preceding rate with thapsigargin ($n = 2$). (*D*) Initial rate of release as fraction of the releasable Ca^{2+}, rather than [Ca^{2+}] per se (see text description). Data points are averages ±SEM using TC vesicles from three different SR preparations.

FKBP12+-incubated and FKBP12-stripped TC (Fig. 2 *D*). The A1-activated Ca^{2+} release from the FKBP12-stripped RyRs remained significantly less than that from FKBP12+-incubated RyRs at all peptide concentrations. The smaller peptide-induced Ca^{2+} release from the FKBP12-stripped vesicles suggests that FKBP12 facilitates the activation of RyRs by the II-III loop peptides.

Addition of peptide NB to one pair of stripped and FKBP12+-incubated vesicle preparations did not evoke Ca^{2+} release (Fig. 2 *C, inset*); the apparent negative release is due to the fact that the release in the presence of thapsigargin became slower with time, so that subtraction of the

latter part of the record from the initial part gave a negative rate.

Effects of peptide A1 on single RyR channels at different cytoplasmic [Ca^{2+}]

Single RyR activity

Peptide A1 (6.5 nM to 32.5 μM) was added to the *cis* chamber, with 250/250 mM Cs^+ (*cis/trans*), a [Ca^{2+}] of 10^{-7}M, 10^{-5}M, or 10^{-4}M (*cis*) and 10^{-3} M (*trans*), 2 mM *cis* Na_2ATP, and 2 or 4 mM $MgCl_2$, with bilayer potentials of −40 mV or +40 mV. A1 had excitatory and inhibitory effects on FKBP12+ native channels (Fig. 3).

RyR activity at −40 mV with 100 nM or 100 μM *cis* Ca^{2+} increased with 650 nM to 32.5 μM *cis* A1, with no change in the maximum open channel conductance (Fig. 3, *A* and *B*). Inhibition by 6.5 μM A1 (Fig. 3 *A*) was apparent at +40 mV, with fewer openings to the maximum conductance. There were substantially fewer openings at +40 mV during strong inhibition by 32.5 μM A1 and long openings (>1 s) to low submaximal conductance levels (Fig. 3 *B*). Channels recovered from the inhibitory effects of the peptide within 15 s after perfusion of the *cis* chamber with peptide-free *cis* solution. Channel activity remained higher than control, especially at −40 mV, for 3–7 min after washout. Activity declined at longer times after washout. Thus inhibition by peptide A1 is rapidly reversible, while activation is less reversible.

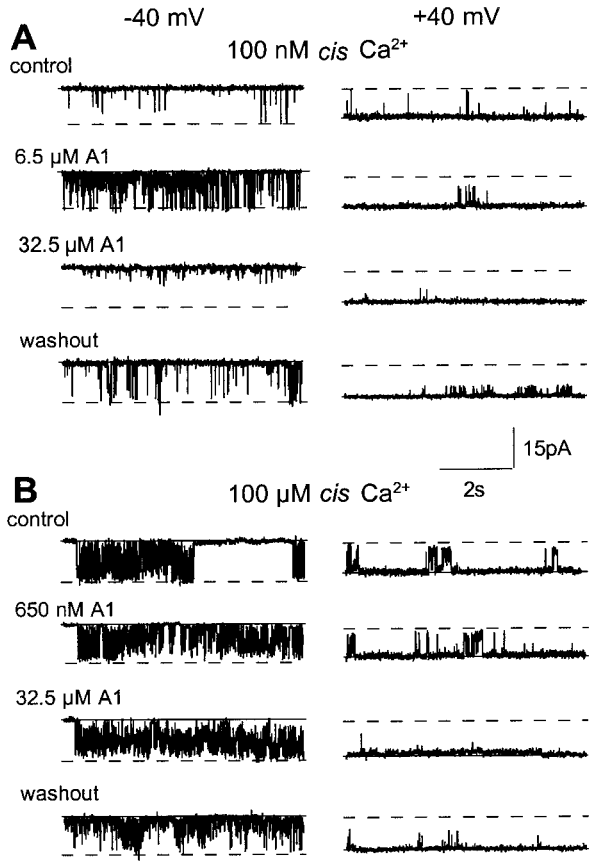

FIGURE 3 Biphasic action of peptide A1 on single native FKBP12+ RyR channels. A1 at 6.5 μM or 32.5 μM increases the activity of recorded at −40 mV, and reversibly depresses activity at +40 mV, with 100 nM *cis* Ca^{2+} (*A*) or 100 μM *cis* Ca^{2+} (*B*). The first records in each panel were obtained under control conditions with 2 mM Na_2ATP and 2 mM $MgCl_2$ in the *cis* solution. The second and third sets of records show activity recorded after 10 s exposure to 6.5 μM or 32.5 μM A1, respectively. The final records were obtained ~4 min after removing peptide A1 from the *cis* chamber by perfusion with 5 vol *cis* solution plus 2 mM Na_2ATP and 2 mM $MgCl_2$. The continuous line in each record shows the closed channel current. The broken line shows the maximum open channel conductance.

Effect of peptide A on the mean current through RyRs

A1 increased mean current through native FKBP12+ RyR channels at −40 mV in 17 of 17 bilayers (100 nM, 10 μM, and 100 μM *cis* Ca^{2+}). The greatest average peptide A1-induced increase (~6-fold) in mean current (I') through RyRs occurred at −40 mV with 100 nM *cis* Ca^2 (Fig. 4 *A* and Table 1).

Average normalized I' at −40 mV increased with A1 between 6.5 nM and 32.5 μM, reaching a maximum with ~6.5 μM peptide with half-maximum concentration between 65 and 650 nM at each *cis* [Ca^{2+}]. I' at +40 mV also increased with [A1] at 100 nM and 10 μM *cis* Ca^{2+} (Fig. 4, *A* and *B*), but fell below control with A1 > 6.5 nM when *cis* [Ca^{2+}] was 100 μM, where inhibition depressed I' below control values with a half-maximum [A1] of ~0.65 μM. It is likely that the decline in activation at higher peptide concentrations under the other conditions can be attributed to inhibition.

Activation by A1 overcame Mg^{2+} inhibition of RyRs. Data for 100 nM and 100 μM *cis* Ca^{2+} were obtained in the presence of 2 mM Na_2ATP and 2 mM $MgCl_2$, with a free Mg^{2+} of 0.6 mM, which inhibits RyRs by >50% (Laver et al., 1997a, b). Data for 10 μM *cis* Ca^{2+} were obtained with either 2 mM $MgCl_2$ (n = 5) or 4 mM $MgCl_2$ (n = 3, with a free Mg^{2+} of 2.1 mM, which inhibits skeletal RyRs by > 90%). Since 6.5 μM A1 caused similar 2.9 ± 0.9-fold increase with 2 mM $MgCl_2$ or 3.2 ± 1.3-fold increase with 4 mM $MgCl_2$, data for the two experiments were pooled for Fig. 4. A1-induced activation was seen in 13 other bilayers (data not shown) with 4 mM $MgCl_2$, 2 mM Na_2ATP, and 100 μM *cis* Ca^{2+}.

Single channel characteristics of A1-activated RyRs

During the strongest activation by 6.5 μM A1 at −40 mV with 100 nM *cis* Ca^{2+}, the open probability (P_o) and open frequency (F_o) were significantly greater than normal, and mean closed time (T_c) was significantly reduced (Table 1). P_o and F_o at −40 mV were similarly increased by 6.5 μM peptide when *cis* [Ca^{2+}] was 100 μM. In contrast, with activating 10 μM *cis* Ca^{2+}, mean open time (T_o) at −40 mV

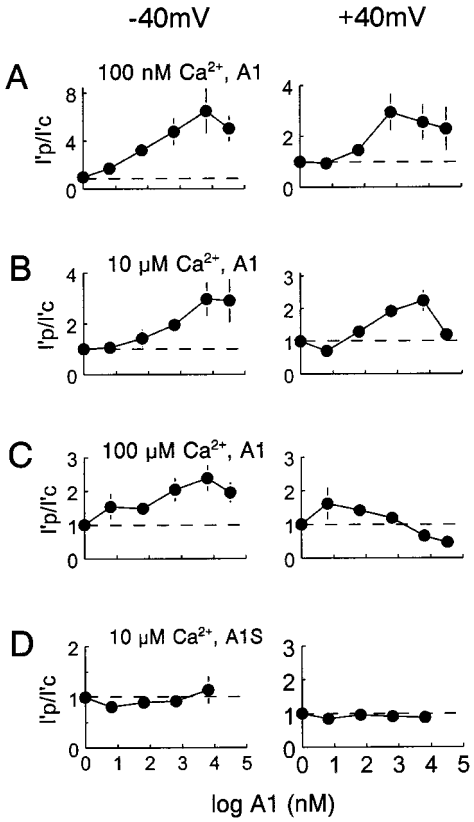

FIGURE 4 Average effects of peptides A1 and A1S on the relative mean current flowing through native FKBP12+ RyRs at −40 mV and +40 mV. Relative mean current ($I'p/I'c$, where $I'p$ is I' in the presence of peptide and $I'c$ is I' under control conditions) is plotted against the logarithm of [peptide A] in nM. Symbols show average $I'p/I'c$ and vertical bars show ±SEM where this is greater than the dimensions of the symbol. Results for A1 were obtained with (*A*) 100 nM *cis* Ca^{2+}, 2 mM Na_2ATP, 2 mM $MgCl_2$ ($n = 5$); (*B*) 10 μM *cis* Ca^{2+}, 2 mM Na_2ATP, 2 mM $MgCl_2$ ($n = 6$) or 4 mM $MgCl_2$ ($n = 3$); (*C*) 100 μM *cis* Ca^{2+}, 2 mM Na_2ATP, 2 mM $MgCl_2$ ($n = 6$). (*D*) Data for peptide A1S were obtained with 10 μM *cis* Ca^{2+}, 2 mM Na_2ATP, 2 mM $MgCl_2$ ($n = 8$).

increased, while F_o was unaffected and indeed fell in two of the five channels. Although the changes in parameter values (I', P_o, F_o, T_o, and T_c) for most individual channels at +40 mV were in the same direction as those at −40 mV, the average changes were significant only with 10 μM *cis* Ca^{2+} (Table 1). Since inhibition by A1 was strongest at +40 mV (Figs. 3 and 4 above), it presumably reduced the degree of activation at this potential.

Removal of peptide A1 enhances RyR activity

Activity often increased further after A1 was perfused out of the *cis* chamber. Average I' and P_o were significantly greater than control (Table 1) after peptide removal, with all *cis* [Ca^{2+}]s at −40 mV, while I', P_o, F_o, and T_o were significantly greater than control, and T_c significantly less, at +40 mV with 100 nM or 10 μM *cis* Ca^{2+} (Table 1). As in the presence of A1, the greatest relative increase in I' after perfusion was at −40 mV with 100 nM *cis* Ca^{2+}, where I' was double that before 32.5 μM A1 washout and ~13-fold greater than control. This result suggests that peptide A is rapidly removed from the blocking site after washout, but that it remains bound to the activation site. Furthermore, the increase in channel activity with A1 removal suggests that the degree of activation in the presence of A1 was suppressed by the simultaneous inhibitory action of the peptide. Data at +40 mV for the three *cis* [Ca^{2+}]s were pooled to more clearly see the effects of activation or inhibition by peptide A1 and peptide washout (Table 2).

There was a significant increase F_o with 6.5 μM A1 (reflecting activation), while F_o fell with 32.5 μM A1 (reflecting inhibition). Washout of 32.5 μM A1 resulted in significant increases in I', P_o, F_o, and T_o, and a significant decrease in T_c (reflecting recovery from inhibition). This result remains consistent with the hypothesis that peptide A is rapidly removed from its blocking site, but not from its activation site, after washout.

Neither scrambled A1 (A1S) nor NB activates RyRs

The strong activation and inhibition of RyR channels induced by peptide A1 were not seen with A1S (Fig. 4 *D*). Similarly, I' was 0.79 ± 0.24 under control conditions and 0.92 ± 0.26 ($n = 6$) after addition of 9.3 μM of NB to the *cis* side of RyRs at +40 mV with 100 μM *cis* Ca^{2+}. P_o, T_o, T_c, and F_o were also unaffected by NB. Curiously, a small inhibition of channel activity was seen with A1S. I' (+40 mV) was less than control in six of seven bilayers with 62 nM and 620 nM *cis* A1S, and in seven of seven bilayers with 6.2 μM *cis* A1S. A fall in I' at −40 mV was also seen in four of seven bilayers after adding 6.2 μM A1S. The average data in Table 3 show that 6.2 μM A1S causes a significant reduction in T_o at −40 mV as well as significant reductions in P_o, F_o, and T_o, or increase in T_c at +40 mV (Table 3).

It is likely that interactions between the positively charged residues in A1 and negative charges in the channel pore cause the strong channel block by A1 (see Discussion below). The clustered positive charges in the C-terminus of A1 presumably provide a high positive charge density that is effective in blocking the channel. The more diffuse charges in A1S may interact less effectively with the same negatively charged sites in the channel pore to give the weak channel block seen in Fig. 4 and Table 3.

Peptide A2 activates and inhibits native FKBP12+ channels

The Ser^{687} Ala substitution did not alter the overall ability of peptide A to activate or inhibit native FKBP12+ RyRs. However, A2 activated RyRs at considerably lower peptide concentrations (AC_{50} between 3.6 and 7.25 nM, Fig. 5), than those required for activation by A1 (AC_{50} of 65–650 nM, Fig. 4 above).

TABLE 1 Average single channel parameters for native FKBP12+ RyRs at −40 or +40 mV exposed to peptide A1

	−40 mV					+40 mV				
	I' (pA)	P_o	F_o (s^{-1})	T_o (ms)	T_c (ms)	I' (pA)	P_o	F_o (s^{-1})	T_o (ms)	T_c (ms)
100 nM Ca^{2+} ($n = 5$)										
Control	0.17 ± 0.03	0.006 ± 0.005	3 ± 2	1.6 ± 0.4	1317 ± 429	0.22 ± 0.04	0.001 ± 0.001	1 ± 1	1.1 ± 0.2	1907 ± 1046
6.5 μM A1	**1.04 ± 0.03***	**0.043 ± 0.021#**	**22 ± 9***	1.6 ± 0.2	**363 ± 287***	0.48 ± 0.14	0.018 ± 0.011	7 ± 5	1.7 ± 0.3	396 ± 116
Washout	**2.11 ± 0.17***	**0.190 ± 0.126#**	**40 ± 10***	3.4 ± 1.6	**25 ± 7#**	**0.74 ± 0.17***	**0.050 ± 0.016***	**23 ± 8***	**2.3 ± 0.3***	**65 ± 24***
10 μM Ca^{2+} ($n = 6$)										
Control	1.92 ± 0.74	0.289 ± 0.138	47 ± 19	3.6 ± 1.7	350 ± 283	0.30 ± 0.06	0.018 ± 0.006	16 ± 5	1.3 ± 0.3	120 ± 53
6.5 μM A1	**3.56 ± 0.71***	**0.445 ± 0.166#**	84 ± 18	**5.9 ± 2.6***	11 ± 7	**0.98 ± 0.18***	**0.097 ± 0.030***	**53 ± 10***	**1.7 ± 0.4***	**24 ± 10***
Washout	**4.97 ± 1.32***	**0.510 ± 0.190***	78 ± 16	**8.6 ± 4.9***	6 ± 2	**1.19 ± 0.21***	**0.131 ± 0.041***	**72 ± 22***	**1.8 ± 0.1***	**22 ± 12***
100 μM Ca^{2+} ($n = 6$)										
Control	1.13 ± 0.17	0.099 ± 0.028	39 ± 7	2.5 ± 0.5	26 ± 14	0.59 ± 0.10	0.052 ± 0.018	26 ± 8	2.3 ± 0.5	89 ± 51
6.5 μM A1	**2.43 ± 0.26***	**0.282 ± 0.051***	**93 ± 12***	2.8 ± 0.2	8 ± 2	0.45 ± 0.22	0.071 ± 0.067	22 ± 17	1.7 ± 0.5	574 ± 243
Washout	**2.82 ± 0.39***	**0.392 ± 0.089***	**106 ± 24***	3.9 ± 0.8	26 ± 19	1.14 ± 0.54	0.113 ± 0.096	25 ± 11	2.5 ± 1.3	209 ± 151

Data are shown as mean ± SE. The number of RyRs is shown in parentheses. Values are shown for control activity (with 2 mM Na_2ATP and 2 mM $MgCl_2$), in the presence of 10 μM A1, and after washout of A1 by perfusion with *cis* solution and addition of 2 mM Na_2ATP and 2 mM $MgCl_2$. Data in bold are significantly different from the control data in the same experimental series.

*Significant according to Student's *t*-test.

#Significant according to the "sign" test.

Although the affinity for A2 was higher than that for A1, the degree of activation induced by the two peptides was similar (~2.5-fold with 10 μM or 100 μM *cis* Ca^{2+}). These results are consistent with the ability of peptide A2 to release Ca^{2+} from native FKBP12+ SR vesicles (above). A2 also overcame inhibition of RyRs by 0.6 mM free Mg^{2+} (with 2 mM $MgCl_2$ in the 10 μM *cis* Ca^{2+} solution, $n = 6$), or 2.1 mM free Mg^{2+} (with 4 mM $MgCl_2$ in the 100 μM *cis* Ca^{2+} solution, $n = 12$).

The affinity of the peptide for the inhibition site was also increased by the Ser^{687} Ala substitution. The IC_{50} at +40 mV was ~360 nM with 10 μM and 100 μM *cis* Ca^{2+}. The *cis* [Ca^{2+}]-dependence of peptide A2-inhibition differed from that with A1. A2 inhibited at +40 mV with 10 μM *cis* Ca^{2+} (dropping I' to ~28% of control, Fig. 5 *A*), and weaker inhibition at 100 μM *cis* Ca^{2+}, with I' falling only to control levels (Fig. 5 *B*).

Minimal peptide A-induced activation in FKBP12-stripped RyRs

In contrast to strong activation of native FKBP12+ channels by peptide A1 (Figs. 3 and 4), activity of FKBP12-stripped RyRs at −40 mV was only slightly greater than normal after exposure to 0.65 μM or 32.5 μM peptide A1 with 100 nM *cis* Ca^{2+} (Fig. 6 *A*), and did not increase after peptide addition with 10 μM *cis* Ca^{2+}, at either −40 mV or +40 mV (Fig. 6 *B*).

The control activity of the FKBP12-stripped channels (Fig. 6, *A* and *B*) was greater than that of native FKBP12+ channels (e.g., Fig. 3 above) as expected (Ahern et al., 1994). More than one channel was active in most bilayers containing FKBP12-stripped RyRs (Fig. 6, *A* and *B*) and long openings to low submaximal conductance levels were apparent, particularly at −40 mV (Fig. 6 *A*). I' (the mean current through the bilayer divided by the number of channels in the bilayer) during control activity at each *cis* [Ca^{2+}] was greater in FKBP12-stripped RyRs than in FKBP12+ RyRs (Table 4).

An increase in activity at −40 mV was seen in 7 of 10 FKBP12-stripped RyRs with 65 nM to 32.5 μM A1 with 100 nM *cis* Ca^{2+}, but was seen in only 3 of the 10 RyRs at +40 mV. On average, I' at −40 mV (100 nM *cis* Ca^{2+}) showed a significant 21% increase after addition of 65 nM to 32.5 μM A1 (Fig. 7 *A*), compared with the 600% increase seen in native FKBP12+ RyRs.

TABLE 2 Average single channel parameters at +40 mV for pooled data obtained with 100 nM, 10 μM, and 100 μM *cis* Ca^{2+}

		+40 mV				
	n	I' (pA)	P_o	F_o (s^{-1})	T_o (ms)	T_c (ms)
Control	17	0.40 ± 0.06	0.023 ± 0.007	14 ± 4	1.5 ± 0.3	669 ± 372
6.5 μM A1	17	1.04 ± 0.03	0.062 ± 0.025	**53 ± 10***	1.7 ± 0.4	331 ± 115
32.5 μM A1	10	0.38 ± 0.12	0.032 ± 0.026	**12 ± 8#**	1.3 ± 0.3	1097 ± 462
Washout	13	**1.02 ± 0.18***	**0.100 ± 0.038#**	**39 ± 10***	**2.2 ± 0.5#**	**107 ± 59***

Data are shown as mean ± SE with the numbers of channels in parentheses. Data in bold are significantly different from the preceding condition, i.e., F_o with 6.5 μM A1 is greater than control, F_o with 32.5 μM A1 is significantly less than with 6.5 μM A1, and F_o after washout is significantly greater than with 32.5 μM A1.

*Significant according to Student's *t*-test.

#Significant according to the "sign" test.

TABLE 3 Average single channel parameters for seven native FKBP12+ RyRs exposed to scrambled A1 (A1S) at +40 mV and −40 mV

	−40 mV					+40 mV				
	I' (pA)	P_o	F_o (s^{-1})	T_o (ms)	T_c (ms)	I' (pA)	P_o	F_o (s^{-1})	T_o (ms)	T_c (ms)
10 μM Ca^{2+}										
Control	1.77 ± 0.69	0.293 ± 0.146	56 ± 19	3.8 ± 0.2	87 ± 61	0.60 ± 0.12	0.044 ± 0.010	40 ± 12	1.3 ± 0.3	34 ± 10
6.2 μM A1S	1.97 ± 0.58	0.289 ± 0.138	47 ± 19	**3.6 ± 1.7#**	345 ± 283	0.53 ± 0.07	**0.018 ± 0.006***	**16 ± 5***	1.3 ± 0.4	**121 ± 53***

Values are shown for control activity (with 2 mM Na_2ATP and 2 mM $MgCl_2$) and in the presence of 6.2 μM A1S. Data are shown as mean ± 1 SE and values in bold are significantly different from the control data.
*Significant according to Student's *t*-test.
#Significant according to the "sign" test.

Activity fell in all bilayers when ≥65 nM A1 was added with 10 μM *cis* Ca^{2+} ($n = 7$) or 100 μM *cis* Ca^{2+} ($n = 3$) and average normalized I' was less than control at both +40 mV and at −40 mV (Fig. 7, *B* and *C*). The fall in I' at −40 mV and +40 mV was significant when 32.5 μM A1 was added with 10 μM *cis* Ca^{2+} and when [A1] was ≥0.65 μM with 100 μM *cis* Ca^{2+}. In contrast to FKBP12-stripped channels, FKBP12+-incubated RyRs were strongly activated by A1 at +40 mV and −40 mV, with 100 nM *cis* Ca^{2+} (Fig. 7 *D*). Therefore, the loss of activation in FKBP12-stripped channels was not due to the incubation procedure. Inhibition without activation was seen in another seven FKBP12-stripped RyRs when 65 nM to 32.5 μM A1 was added with 100 μM *cis* Ca^{2+}, 2 mM Na_2ATP, and 4 mM $MgCl_2$. The results confirm the Ca^{2+} release studies and show that activation of native RyRs by peptide A1 depends on the presence of the FK506-binding protein.

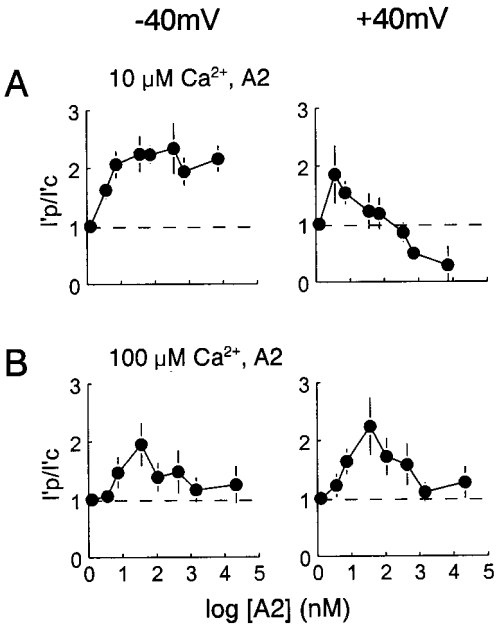

FIGURE 5 Peptide A2 activates native FKBP12+ RyRs at −40 mV and inhibits the RyRs at +40 mV. Relative mean current ($I'p/I'c$, where $I'p$ is I' in the presence of peptide and $I'c$ is I' under control conditions) is plotted against the logarithm of peptide A2 concentration (log[A2]) in nM. Symbols show average $I'p/I'c$ and vertical bars show ±1 SEM where this is greater than the dimensions of the symbol. Results for A2 were obtained with (*A*) 10 μM *cis* Ca^{2+}, with 2 mM Na_2ATP and 2 mM $MgCl_2$ ($n = 6$); (*B*) 100 μM *cis* Ca^{2+} with 2 mM Na_2ATP and 4 mM $MgCl_2$ ($n = 12$).

Peptide A block of FKBP+ and FKBP-stripped RyRs

Effects of ATP and Mg^{2+}

The block of RyRs by peptide A was unexpected because ≥6.5 μM of the peptide caused significant ruthenium red-sensitive Ca^{2+} release from TC vesicles. The recording conditions were varied to ascertain whether, in addition to depending on *cis* [Ca^{2+}], channel block by peptide A was influenced by cytoplasmic (*cis*) ATP or Mg^{2+}. Block was seen with 100 μM *cis* Ca^{2+} in the absence of ATP or Mg^{2+} ($n = 11$) or with 2 mM ATP (without Mg^{2+}, $n = 6$). Thus channel block appeared to be independent of ATP or Mg^{2+} in the *cis* solution.

Effect of permeant ions on the inhibition of RyRs by peptide A1

Inhibition of RyR activity by peptide A was stronger at +40 mV than at −40 mV (Figs. 3 and 4). This apparent membrane potential-dependence might have been due to an effect of membrane potential per se on peptide binding and channel block, or it could be due to permeant cations entering the pore from the opposite side of the channel (i.e., the *trans* bath). The latter possibility would suggest a blocking mechanism in which the peptide binds within the channel pore and is displaced by ion flow from the *trans* chamber. To explore this possibility, we measured the effect of varying the concentration of permeant ions in the *trans* chamber (at constant membrane potential) on the inhibition of native FKBP12+ RyR channels by *cis* peptide. In these experiments the bilayers were composed of only neutral lipids (see Methods) to minimize bilayer surface potentials and possible effects of the *trans* solution ionic strength on surface potential and peptide binding. If charged lipids were used, changes in the ionic composition of the *trans* bath could alter peptide binding even if the binding site was not in the pore. The *trans* concentration of the permeant cation, Cs^+, but not the impermeant cation, $choline^+$, had a major effect on the strength of peptide inhibition (Fig. 8).

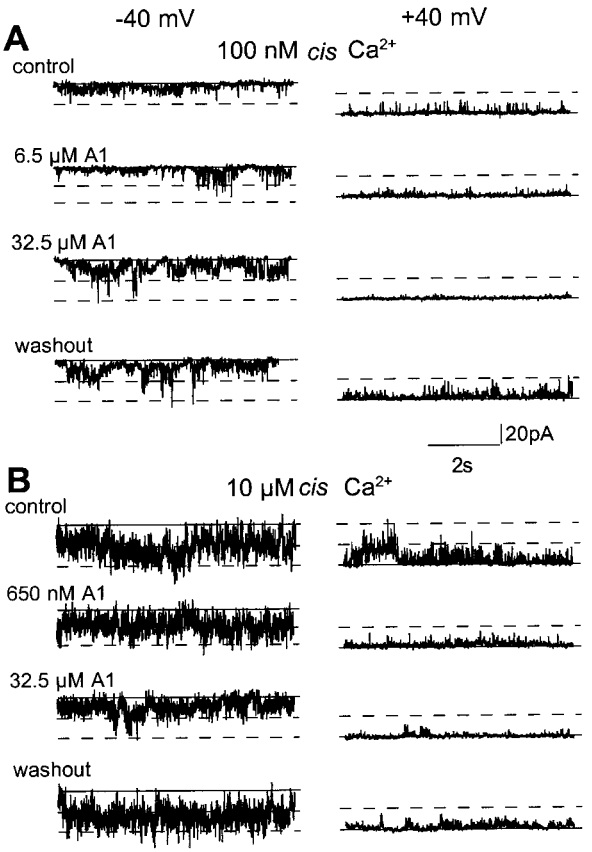

FIGURE 6 FKBP12-stripped RyRs are not significantly activated by peptide A1. (*A*) Records from a bilayer with 100 nM *cis* Ca^{2+}. (*B*) records from a second bilayer with 10 μM *cis* Ca^{2+}. The *cis* solution also contained 2 mM Na_2ATP and 2 mM $MgCl_2$. The first records in each panel were obtained under control conditions. The second and third records show activity after 10 s exposure to 6.5 μM or 32.5 μM A1, respectively. The final records were obtained ~4 min after removing A1 by perfusion with *cis* solution plus 2 mM Na_2ATP and 2 mM $MgCl_2$. Two RyR channels were present in each bilayer. The continuous line shows the zero current level. The broken lines indicate the maximum open conductance of one (*first line*) or two (*second line*) channels.

RyR activity at 0 mV was not altered by 4 μM *cis* A1, but was strongly inhibited by 8 μM A1 (Fig. 8 *A, trace 3*). Channel activity recovered when the bilayer was perfused with solution lacking the peptide and the current direction reversed when the Cs^+ concentration in the *trans* chamber was increased from 50 mM to ~1000 mM (at 0 mV, Fig. 8 *A, trace 4*). The channel became relatively insensitive to A1 block and remained active with 32 μM A1 (Fig. 8 *A, trace 5*). A similar reduction in peptide block after increasing *trans* Cs^+ to 1000 mM was seen in four of four experiments. In contrast, in two experiments where 1000 mM $choline^+$ was added to the *trans* solution (to give a similar increase in ionic strength to 1000 mM Cs^+), 8 μM A1 blocked the RyR in the usual way (Fig. 8 *B, trace 7*). The effect of the cation composition of the *trans* solution on the half-inhibiting concentrations of A1 are summarized in Table 5.

Increasing the concentration of the permeant cation (Cs^+) in the *trans* solution from 50 mM to 1000 mM caused a sixfold increase in the concentration of A1 required for 50% block of the RyR. In contrast, there was a 40% reduction in the [A1] required for half-maximum block in the presence of 1000 mM $choline^+$ (see also Fig. 8), possibly because the *trans* Cs^+ concentration was reduced to 30 mM.

TABLE 4 Average control mean current (*I′*) through FKBP12+ (native or incubated) or FKBP12-stripped RyRs at each of the three *cis* Ca^{2+} concentrations listed

	100 nM	10 μM	100 μM
cis [Ca^{2+}]	*I′* (pA)	*I′* (pA)	*I′* (pA)
FKBP12+ native			
−40 mV	0.17 ± 0.03	1.77 ± 0.69	1.13 ± 0.17
+40 mV	0.22 ± 0.04 (6)	0.63 ± 0.17 (7)	0.59 ± 0.10 (6)
FKBP12-stripped			
−40 mV	**1.23 ± 0.36***	**3.85 ± 0.64***	**4.02 ± 1.28***
+40 mV	**1.53 ± 0.30*** (10)	**2.54 ± 0.58*** (8)	**2.14 ± 0.84*** (3)
FKBP12+ incubated			
−40 mV	**0.48 ± 0.11*#**		
+40 mV	**0.46 ± 0.06*#** (4)		

I′ is the mean current across the bilayer divided by the number of RyR channels in the bilayer. Data are shown as mean ± 1 SE with the number of bilayers given in parentheses.
*Significantly greater (Student's *t*-test) than values obtained in native FKBP12+ RyRs at the same potential and *cis* [Ca^{2+}].
#FKBP12+ incubated values are also significantly less than the equivalent FKBP-stripped data.

Channel openings to submaximal conductances are resistant to inhibition by peptides A1 and A2

FKBP12+ channels

The reduced channel activity (and *I′*) produced by adding >4 μM A1 was due to fewer channel openings (Table 2), to a reduction in the number of openings to the maximum conductance in native FKBP12+ (Fig. 3; Figs. 8 and 9), and in FKBP12+-incubated channels. The native FKBP12+ RyR in Fig. 9 showed long openings (lasting for >20 ms) to the maximum conductance and to several submaximal conductance levels under control conditions at +40 mV (Fig. 9 *A*). When 6.5 μM peptide was added, there were only occasional brief openings to the high conductance levels, although long openings to submaximal conductance levels remained and were longer than those in the control record (Fig. 9 *B*). Channel openings to the maximum conductance recovered when the peptide was perfused out of the *cis* chamber (Fig. 9 *C*). The maximum conductance and three of the submaximal levels (at ~11, 33, and 67% of the maximum conductance) that could be seen under all conditions are shown by the broken lines on the records and by the arrows on the histograms. Similar effects of peptide block on openings to the maximum conductance were seen at all *cis* [Ca^{2+}] tested, and were seen to a lesser extent at −40 mV.

FKBP12-stripped channels

The effect of peptide A in preferentially blocking channel openings to maximum conductance levels was also apparent

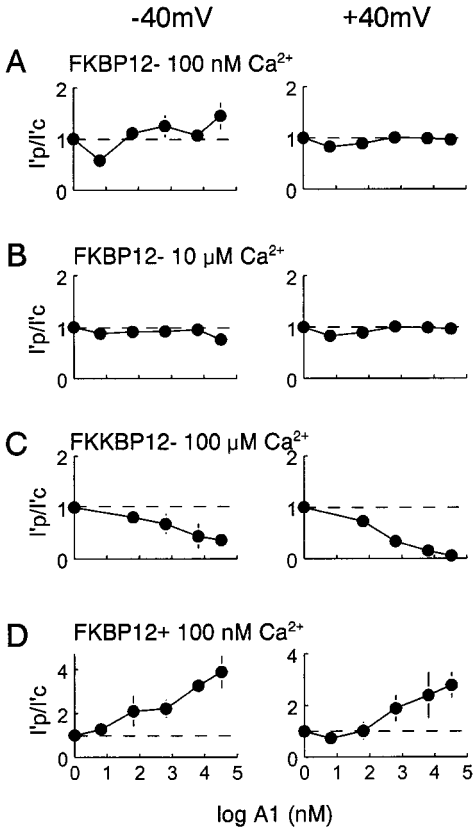

FIGURE 7 Average effects of peptide A1 on the mean current flowing through FKBP12-stripped RyRs and FKBP12+ incubated RyRs at +40 mV and −40 mV. Relative mean current ($I'p/I'c$, where $I'p$ is I' in the presence of peptide and $I'c$ is I' under control conditions) is plotted against the logarithm of [peptide A1] in nM. Symbols show average $I'p/I'c$ and vertical bars show ±1 SEM where this exceeds the dimensions of the symbol. Results with FKBP12-stripped RyRs were obtained with 2 mM Na_2ATP and 2 mM $MgCl_2$, and (*A*) 100 nM *cis* Ca^{2+} ($n = 10$); (*B*) 10 μM *cis* Ca^{2+} ($n = 8$); (*C*) 100 μM *cis* Ca^{2+} ($n = 4$). (*D*) Data for FKBP12+ incubated RyRs were obtained with 100 nM *cis* Ca^{2+}, 2 mM Na_2ATP, and 2 mM $MgCl_2$ ($n = 3$).

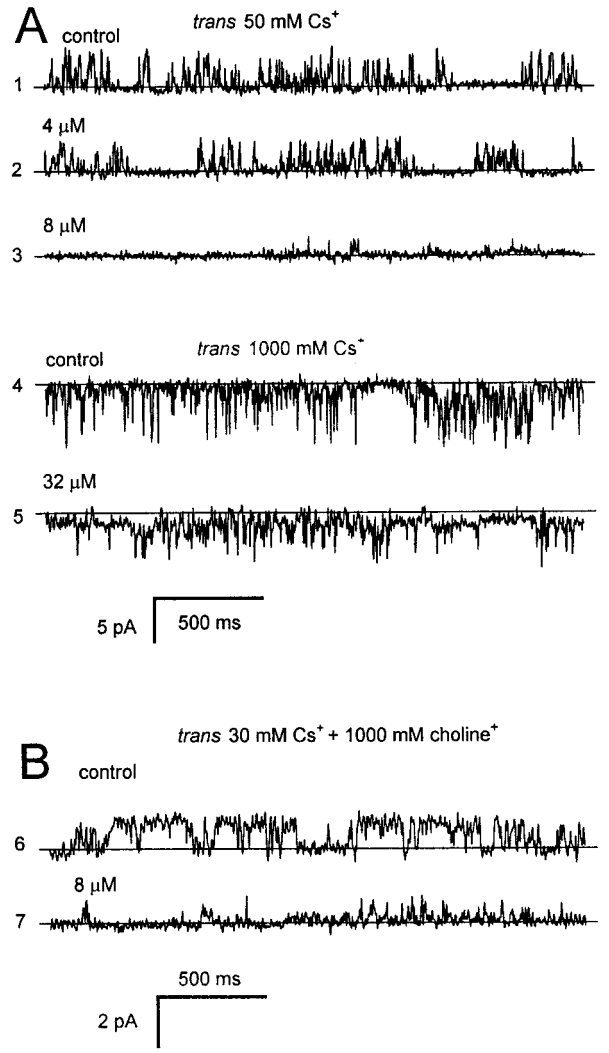

FIGURE 8 Inhibition of RyR activity at 0 mV by peptide A1 in the *cis* solution is relieved by increasing the permeant ion concentration in the *trans* solution. Bilayers contained 80% phosphatidylethanolamine and 20% phosphatidylcholine. The *cis* solution contained (in mM): 230 CsMS, 20 CsCl, 0.1 $CaCl_2$, 2 Na_2ATP, and 2 $MgCl_2$. (*A*, *Traces 1–3*) Channel activity with 50 mM *trans* Cs^+ (30 mM CsMS + 20 mM CsCl) so that Cs^+ flowed from the *cis* to *trans* bath. Addition of 8 μM A1 almost abolished RyR activity. *Traces 4* and *5* were from the same channel at 0 mV after perfusion with A1-free solution and increasing *trans* [Cs^+] to 1000 mM by *trans* addition of 4 M CsMS, so that Cs^+ flow was *trans* to *cis*. Under these conditions, 32 μM A1 produced relatively little inhibition. (*B*) In separate experiments, 1000 mM choline$^+$, (an RyR impermeant cation) was added to the *trans* solution initially containing 50 mM Cs^+. Adding choline$^+$ diluted the *trans* [Cs^+] to 30 mM, reducing RyR conductance and current amplitude. In contrast to 1000 mM *trans* Cs^+, the 1000 mM *trans* choline$^+$ did not reduce peptide A1 block of RyRs.

in FKBP12-stripped channels that demonstrated considerable submaximal conductance activity in the absence of peptide. As previously reported for FKBP12-stripped channels (Ahern et al., 1994, 1997a), three major submaximal conductance levels were apparent in the FKBP12-stripped channels. In the channel shown in Fig. 9, *D–F*, these levels were at ~17, 33, and 67% of the maximum conductance. Only very brief openings (<1 ms) to the maximum conductance were seen under control conditions, although long openings to the 67% level were apparent. Fewer, briefer openings to the 67% level were observed with 6.5 μM peptide, although long openings to the 17 and 33% levels remained (Fig. 9 *E*). Openings to the 67 and 100% levels recovered when the peptide was perfused out of the *cis* chamber (Fig. 8 *F*). Similar conductance levels and peptide-induced block of openings to the maximum conductance were seen in FKBP12-stripped channels at −40 mV, and with 100 nM and 100 μM *cis* Ca^{2+}.

Incidental observations: RyR activation by ATP and inhibition by Mg^{2+}

Addition of 2 mM ATP induced the expected increase in average I' through native FKBP12+ channels at both +40 mV and −40 mV with 100 μM *cis* Ca^{2+} ($n = 20$, Fig. 10). Addition of 4 mM $MgCl_2$ (2.1 mM free Mg^{2+}) then reduced I' at positive and negative potentials, but to levels that

TABLE 5 The effect of the permeant ion concentration in the *trans* chamber on the ability of peptide A to block RyR channels from the *cis* side

trans [cation]	*n*	[A1] For Half-Maximum Inhibition
50 mM Cs^+	6	5.0 ± 0.4 μM
1000 mM Cs^+	4	24.0 ± 5.0 μM
30 mM Cs^+ + 1000 mM choline$^+$	2	2.8 ± 0.2 μM

Experimental conditions and protocols are described in the text and in the legend to Fig. 8.

remained higher than those before addition of ATP. The response to both ATP and 4 mM $MgCl_2$ was similar in the 20 normal and 16 FKBP12-stripped channels, although channel activity fell to levels that were not significantly different from control when 4 mM $MgCl_2$ was added to the FKBP12-stripped channels at +40 mV (Fig. 10 *B*). If 2 mM $MgCl_2$ was added simultaneously with 2 mM Na_2ATP (with 0.6 mM free Mg^{2+}), channel activity remained at levels that were not significantly different from control or greater than control (Table 6).

Since 2 mM ATP alone activated the channels (Fig. 10), channel activity with 2 mM Na_2ATP plus 2 mM $MgCl_2$ must have been depressed from the ATP-activated level. The reduction in activity with 0.6 mM free [Mg^{2+}] does not appear to be significantly less than the block with 2.1 mM Mg^{2+}, and the block with either Mg^{2+} concentration is considerably less in the presence of ATP than it is when ATP is absent (Laver et al., 1997a), confirming previous observations in cardiac RyRs (Xu et al., 1996). No consistent differences were noted between 1) the native FKBP12+ and FKBP12-stripped channels, or 2) between the effects of ATP and Mg^{2+} at different *cis* Ca^{2+} concentrations.

DISCUSSION

We show here that peptide A (corresponding to the N terminal of the DHPR II-III loop), at concentrations from 65 nM to 32.5 μM, activates native RyR channels at −40 mV with *cis* [Ca^{2+}]s of 100 nM, 10 μM, and 100 μM. The peptide also inhibited channel activity in native RyRs and, at >4 μM, reduced the mean current at +40 mV to less than control levels when *cis* [Ca^{2+}] was 100 μM. Activation by peptide A was expected because it has been shown that the peptide increases [^{3}H]ryanodine binding to, and releases Ca^{2+} from, SR vesicles (El-Hayek et al., 1995). The blocking action of the peptide was not expected from previous single channel studies on longer segments of the II-III loop (Lu et al., 1995), although a decline in the rate of peptide-activated Ca^{2+} release from SR is apparent with higher concentrations of a fragment of the peptide (El-Hayek and Ikemoto, 1998).

Peptide A activation of the skeletal RyR

Peptide A activation overcame Mg^{2+} block of RyR activity. Mg^{2+} block reduced RyR activity and suppressed Ca^{2+} release through the channel in resting muscle (Lamb and Stephenson, 1991). Peptide A activated RyRs in the presence of ~0.6 mM free Mg^{2+} in Ca^{2+} release experiments, or 0.6 mM to 2.1 mM free Mg^{2+} in single channel experiments (with 10^{-7} to 10^{-4} M Ca^{2+}). Thus, peptide A-induced activation mimics ECC insofar as it can overcome Mg^{2+}-inhibition of RyR activity.

The degree of activation of the RyR by peptide A was not as large as expected for the primary trigger of RyR opening during ECC. Channel open probability (P_o) with 0.65–6.5 μM peptide remained well below 1.0 (Table 1), while the rate of Ca^{2+} release from TC in our experiments, and in the faster release in stop-flow experiments (El-Hayek and Ikemoto, 1998), remain slower than Ca^{2+} release during ECC (Melzer et al., 1987). The lower-than-expected activation could indicate that a conformational change in the II-III loop occurs during ECC, but does not occur when the peptide is isolated from the remainder of the DHPR and is not under the influence of the T-tubule membrane potential. Alternatively (or in addition), the relatively small increase in I' and P_o could be due to the strong concurrent inhibition. Although inhibition per se was not apparent in SR Ca^{2+} release, inhibition could have reduced the degree of activation (as indicated by the increased activity after removal of peptide A from the *cis* chamber).

It is likely that peptide A activation of the RyR depends on the highly positively charged residues in the C half of the peptide. A smaller II-III loop peptide containing these arginine and lysine residues (Arg Lys Arg Arg Lys Met Ser Arg Gly Leu), increases ^{3}H-ryanodine binding and releases Ca^{2+} from SR (El-Hayek and Ikemoto, 1998; Dulhunty et al., 1999). Thus it is likely that it is this segment of the II-III loop that binds to skeletal RyRs at residues 1076–1112 (Leong and Maclennan, 1998). Skeletal type ECC also requires region D3, residues 1872–1923 (Nakai et al., 1998a), and perhaps region D2 (1342–1403, Yamazawa et al., 1997) of the RyR. The involvement of these diverse regions of the RyR indicates a complex transduction pathway through the channel protein between its interaction with the DHPR and the ion channel pore. This is not surprising, given the size and complex structure of the protein (Radermacher et al., 1994; Orlova et al., 1996; Wagenknecht and Radermacher, 1997; Wagenknecht et al., 1997).

Importance of Ser^{687} in II-III loop activation of RyRs

In our studies, enhanced peptide-induced Ca^{2+} release from TC and activation of single RyRs at lower peptide concentrations were seen with the Ser^{687} Ala substitution. This is in contrast to the abolition of activation seen with the same substitution in the full II-III loop (Lu et al., 1995). However, Ser^{687} Ala substitution in the entire DHPR α_1 subunit does not alter the ability of the DHPR to support skeletal-type ECC (Nakai et al., 1998b). The reasons for these conflicting

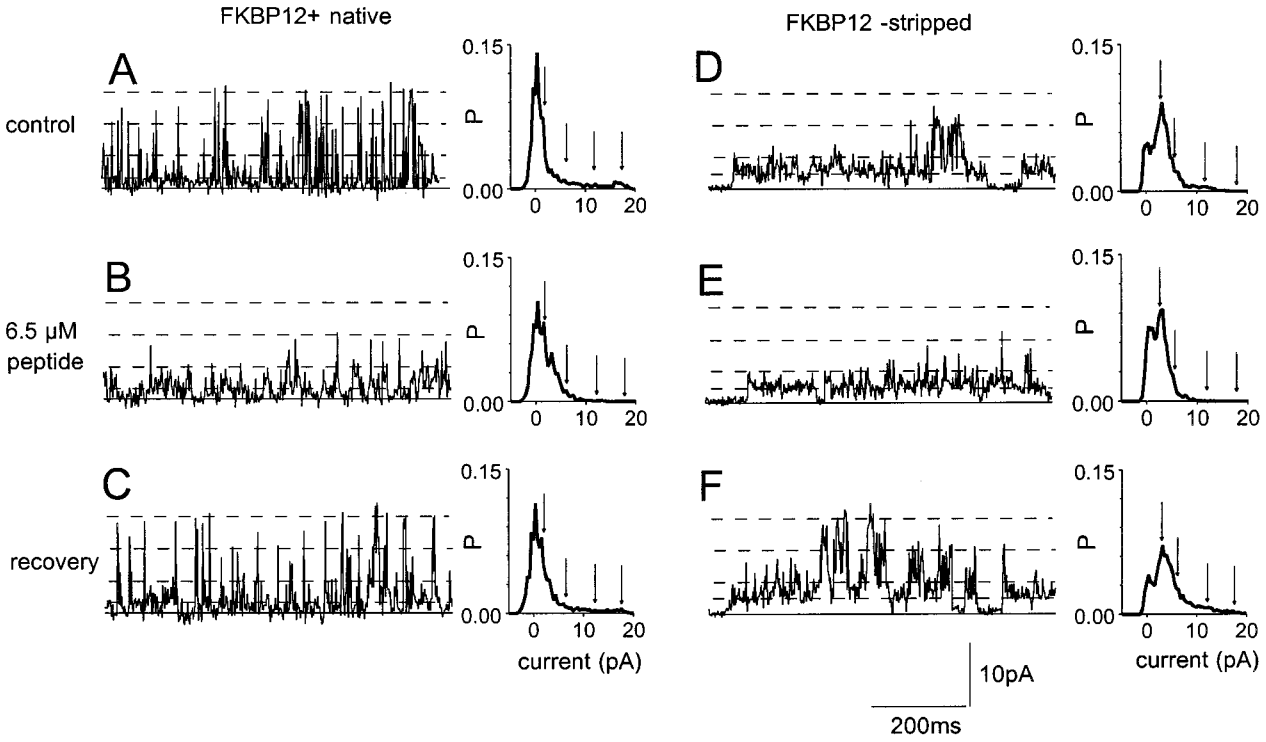

FIGURE 9 Effects of block by peptide A1 on conductance levels in single native FKBP12+ (*A–C*) and FKBP12-stripped (*D–F*) channels at +40 mV, in the presence of 10 μM *cis* Ca^{2+}. The upper records (*A* and *D*) show control activity, the middle records (*B* and *E*) were obtained after adding 6.5 μM A1 to the *cis* solution, and the lower records (*C* and *F*) show recovery of high conductance activity after A1 perfusion out of the *cis* chamber. The continuous lines show the zero current for each channel. All-points histograms, showing the probability of activity to current levels (in pA), are shown beside each record. The arrows on the histograms point to current levels [identified by *I* in the records (*broken lines*) and as peaks or discontinuities in the histograms (*arrows*)], that are common to all conditions. These are the maximum conductance and three submaximal conductance levels for the FKBP12+ channel and the FKBP12-stripped channel.

results are not clear. However, the Ser^{687} Ala substitution could well produce a structural change that prevents the full II-III loop from activating the RyR, but that enhances activation by the shorter peptides. Enhanced activation may not have been detected within the resolution of the ECC studies (Nakai et al., 1998b).

The FK506 binding protein

The ability of peptide A to activate RyRs was substantially reduced in FKBP12-stripped RyRs. The removal of FKBP12 reduces the number of RyR openings to the maximum conductance, but does not alter the regulation of the channel by Ca^{2+} (Ahern et al., 1997b), ATP, Mg^{2+}, or caffeine (see Results). The influence of FKBP12 on channel activation by A1 is unique among these ligands, which supports suggestions that FKBP12 plays a role in RyR activation during ECC (Ahern et al., 1994, 1997a; Brillantes et al., 1994; Mayrleitner et al., 1994; Lamb and Stephenson, 1996).

The putative FKBP12 binding domain at 2407–2520 (Cameron et al., 1997) is located on the surface of the RyR that opposes the T-tubule membrane (Wagenknecht et al., 1997). Four FKBP12 molecules bind to each RyR, i.e., one per subunit (Jayaraman et al., 1992; Timerman et al., 1993; Wagenknecht et al., 1996, 1997). The II-III loop binding domain must be located on the same surface of the RyR to enable the DHPR to bind to the RyR. Since skeletal muscle DHPRs are clumped into tetrads, which oppose every second RyR (Block et al., 1988), each subunit of every second RyR is likely to interact with the II-III loop of one of the DHPRs in a tetrad. The T-tubule opposing surface of each subunit of the RyR must contain an FKBP12 binding site and a II-III loop binding site. An interaction between FKBP12 binding and activation of RyRs by the II-III loop has been suggested by the fact that FK506 can disrupt depolarization-induced Ca^{2+} release from the SR (Lamb and Stephenson, 1996).

Physiological interactions between the DHPR and the RyR during ECC

It is not known whether the II-III loop is bound to the RyR in vivo or binding occurs only during ECC. In the latter case, binding alone could be sufficient to activate the RyR although, as mentioned previously, the activation produced by peptide binding is not as strong as might be expected. However, there is evidence that a complex can be formed between the RyR and DHPR (Marty et al., 1994; Murray

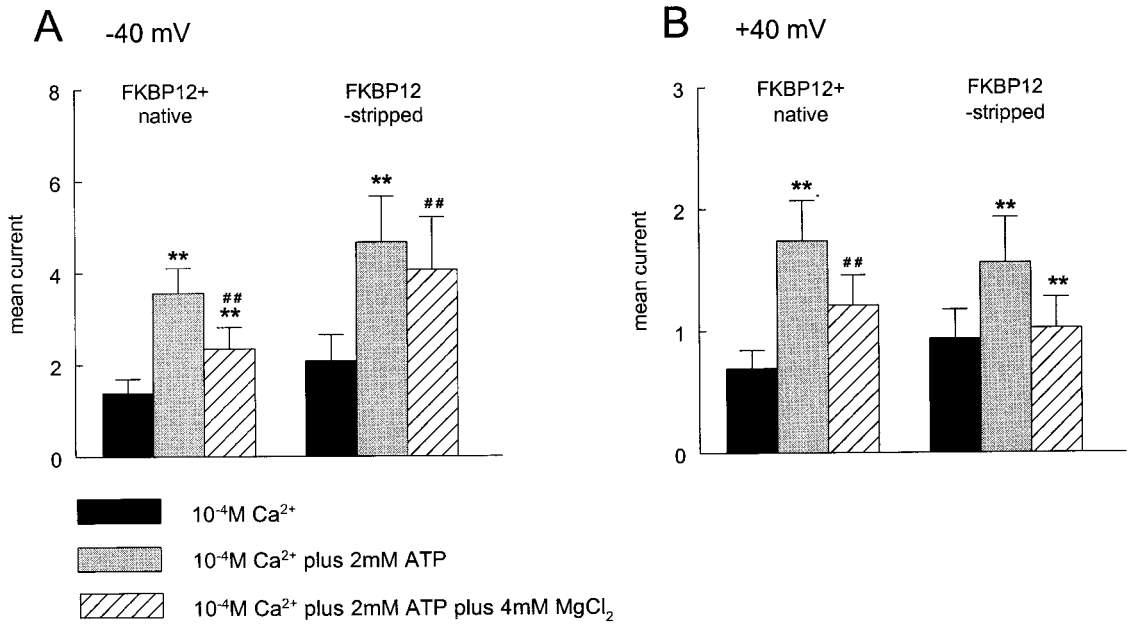

FIGURE 10 Histograms compare the effects of Na_2ATP and $MgCl_2$ on the mean current through native FKBP12+ and FKBP12-stripped channels. Control channel activity was recorded in the presence of 10^{-4} M Ca^{2+} (*black bars*). Activity after adding 2 mM ATP is shown in the gray bars and activity with 2 mM Na_2ATP plus 4 mM $MgCl_2$ is shown in the cross-hatched bars. Data are given as mean ± SE. The asterisks (**) indicate that the mean value is significantly different from that for the preceding condition, $p < 0.01$. The cross-hatch symbols (##) indicate that mean current with 2 mM Na_2ATP plus 4 mM $MgCl_2$ is significantly different from the that under control conditions, $p < 0.01$.

and Ohlendieck, 1998). If there is a stable II-III loop-RyR complex, then RyR activation during ECC could depend on a conformational change in the II-III loop being transmitted, through the DHPR/RyR interaction site, to the RyR.

Although studies with synthetic peptides and RyRs in bilayers or vesicles clearly show that peptide A can activate the calcium release channel, apparently conflicting results have been obtained from ECC studies with dysgenic myotubes expressing chimeric DHPRs. It is clear that the skeletal ECC (independent of external Ca^{2+}) requires the skeletal II-III loop and will not proceed if the loop contains the cardiac sequence (Tanabe et al., 1990). However, when chimeras are constructed with parts of the II-III loop, skeletal-type ECC proceeds when the A portion contains either the cardiac or skeletal sequence (Nakai et al., 1998b). Skeletal ECC has an absolute requirement for the skeletal sequence in residues 725–742 (encompassed in the C portion of the II-III loop according to El-Hayek et al., 1995). Lu et al. (1994, 1995) found that both the cardiac and skeletal II-III loops increased ryanodine binding to SR vesicles and activated RyR channels, suggesting that both the cardiac and skeletal II-III loops bind to the skeletal RyR, and in agreement with the ECC studies. The II-III loops presumably bind to the RyR at the A region, which contains several arginine and lysine residues in both the skeletal and cardiac isoforms.

TABLE 6 Average control mean current (I') through FKBP12+ (native) or FKBP12-stripped RyRs at each of the three *cis* Ca^{2+} concentrations listed

		100 nM	10 μM	100 μM
cis [Ca^{2+}]		I' (pA)	I' (pA)	I' (pA)
FKBP12+ native				
+40 mV	Control	0.34 ± 0.04 (6)	0.75 ± 0.04 (7)	0.45 ± 0.08 (6)
	ATP/Mg	0.22 ± 0.04	0.63 ± 0.17	0.59 ± 0.10
−40 mV	Control	0.15 ± 0.04	0.64 ± 0.17	0.72 ± 0.16
	ATP/Mg	0.17 ± 0.03	1.77 ± 0.69	1.13 ± 0.17
FKBP12-stripped				
+40 mV	Control	1.19 ± 0.17 (8)	1.87 ± 0.46 (8)	2.03 ± 0.56 (3)
	ATP/Mg	1.37 ± 0.25	**2.53 ± 0.58***	2.14 ± 0.84
−40 mV	Control	1.68 ± 0.55	2.86 ± 0.73	2.65 ± 0.52
	ATP/Mg	1.41 ± 0.40	**3.85 ± 0.64***	4.02 ± 1.37

I' is the mean current across the bilayer divided by the number of RyR channels in the bilayer. Data are shown as mean ± 1 SE with the number of bilayers given in parentheses.

*Significantly greater (Student's *t*-test) than control values.

One hypothesis that could explain most observations is that the positively charged A region of the II-III loop binds to the RyR, causing an increase in RyR activity. Full activation of the RyR requires a conformational change at the binding site, which is initiated by the voltage sensor in the S4 segment of the DHPR and is transmitted through the C region (725–742) of the II-III loop. Either the skeletal or cardiac sequence of the II-III loop binds to (or interacts with) the skeletal RyR. However, skeletal-type ECC requires transmission of T-tubule depolarization to the II-III loop/RyR interaction site, and this can only proceed if residues 725–742 contain the skeletal DHPR sequence.

Peptide A inhibition of the skeletal RyR

The peptide inhibition site is distinct from the II-III loop activation site because 1) inhibition is greatest at 100 μM *cis* Ca^{2+}, while activation is greatest at 100 nM *cis* Ca^{2+}; 2) inhibition, but not activation, depends on the direction of current flow; and 3) unlike activation, inhibition is not disrupted by removing FKBP12. The fact that inhibition by *cis* peptide A was reduced when Cs^+ flows from *trans* to *cis* is consistent with the peptides blocking by binding to the pore or vestibule of the RyR, since Cs^+ could enter the pore from the *trans* bath and compete with the peptide for its binding site. This hypothesis is supported by the fact that high *trans* [choline$^+$], which does not pass through RyR channels, did not affect *cis* peptide inhibition. The sensitivity of peptide block to the flow of permeant cations may also account for its voltage-dependence, since at negative potentials the electric field in the pore will favor cation permeation from the *trans* side, whereas positive potentials will oppose it.

In contrast to peptide A, the full-length DHPR II-III loop has not been reported to inhibit RyR activity (Lu et al., 1994, 1995). Failure of the full-length II-III loop to block can be explained if the blocking site is in the channel pore, since the bulk of the longer peptide could restrict its access to the blocking site. The observation is consistent with the hypothesis that there are separate inhibition and activation sites.

Permeant ions flowing from the opposite side of a channel have been shown elsewhere to reduce the binding of pore blocking peptides [e.g., charybdotoxin block of the Ca^{2+}-activated K^+ channel (MacKinnon and Miller, 1988)]. A toxin that blocks the K^+ channel pore also blocks RyRs, possibly because positively charged arginine and lysine residues in the peptides bind to negative charges near the channel pore (Mead et al., 1998). Peptide A, also rich in arginine and lysine residues, may bind to the RyR at a site similar to the toxin binding site.

Two factors that need to be considered in developing a model for peptide binding in the channel pore are 1) inhibition depends on *cis* [Ca^{2+}] and is greatest at 100 μM *cis* Ca^{2+}; and 2) inhibition preferentially targeted maximal conductance openings, while leaving openings to submaximal conductances intact. The blocking mechanism must differ from ryanodine block, which causes equal depression of all conductance levels (Ahern et al., 1997a). The sensitivity of peptide inhibition to direction of flow of permeant ions may account for the fact that inhibition was not apparent in vesicle experiments, since Ca^{2+} flow from the lumen to cytoplasm (*trans* to *cis*) would reduce peptide-induced inhibition. The *cis* [Ca^{2+}]-dependence of inhibition would also reduce the efficacy of inhibition in the vesicle experiments since the extravesicular [Ca^{2+}] was considerably less than 100 μM during maximum rates of release. Although inhibition dominated the effect of peptide A on RyRs in bilayers, it might not reflect a physiological action of the DHPR, since the II-III loop in vivo is physically constrained by the DHPR's location in the T-tubule membrane and may not be free to enter the channel pore. However, inhibition must be considered when studying the action of the II-III loop, or loop peptides, on Ca^{2+} release from SR or on single RyR channels.

In conclusion, we have shown that peptides corresponding to an amino acid sequence in the N-terminal region of the II-III loop of the skeletal muscle DHPR activate ryanodine-sensitive Ca^{2+} release from SR vesicles and activate single RyR channels incorporated into lipid bilayers. Study of RyR channel activation by the peptide is complicated by a competing strong inhibitory action of the peptide. The results show that activation of RyRs by the peptide is not dependent on Ser^{687} in the DHPR II-III loop and that activation of the RyR by the peptide is facilitated when FKBP12 is bound to the RyR. These observations suggest that activation of the RyR by the DHPR II-III loop requires a complex sequence of signals passing from the II-III loop binding site to the RyR channel pore. The inhibitory action of peptide binding could provide a useful tool to probe the RyR pore, but inhibition is unlikely to be relevant to RyR function in vivo.

The authors are grateful to Joan Stivala, Glen Whalley, and Bernie Keys for their assistance.

Professor Gallant was supported by grants from the National Institutes of Health and National Science Foundation. Dr. D. R. Laver was supported by a grant from the Australian National Health and Medical Research Council.

REFERENCES

Ahern, G. P., P. R. Junankar, and A. F. Dulhunty. 1994. Single channel activity of the ryanodine receptor calcium release channel is modulated by FK506. *FEBS Lett.* 352:369–374.

Ahern, G. P., P. R. Junankar, and A. F. Dulhunty. 1997a. Subconductance states in single-channel activity of skeletal muscle ryanodine receptors after removal of FKBP12. *Biophys. J.* 72:146–162.

Ahern, G. P., P. R. Junankar, and A. F. Dulhunty. 1997b. Ryanodine receptors from rabbit skeletal muscle are reversibly activated by rapamycin. *Neurosci. Lett.* 225:81–84.

Block, B. A., T. Imagawa, K. P. Campbell, and C. Franzini-Armstrong. 1988. Structural evidence for direct interaction between the molecular components of the transverse tubule/sarcoplasmic reticulum junction in skeletal muscle. *J. Cell Biol.* 107:2587–2600.

Brillantes, A.-M. B., K. Ondrias, A. Scott, E. Kobrinsky, E. Ondriasova, M. C. Moschella, T. Jayaraman, M. Landers, B. E. Ehrlich, and A. R. Marks. 1994. Stabilization of calcium release channel (ryanodine receptor) function by FK506-binding protein. *Cell*. 77:513–523.

Cameron, A. M., F. C. Nucifora, E. T. Fung, D. J. Livingston, R. A. Aldape, C. A. Ross, and S. H. Synder. 1997. FKBP12 binds the inositol 1,4,5-trisphosphate receptor at leucine-proline (1400–1401) and anchors calcineurin to this FK506-like domain. *J. Biol. Chem.* 272: 27582–27588.

Dulhunty, A. F., S. M. Pace, and S. M. Curtis. 1999. Residues in the skeletal DHPR II-III loop that activate or inhibit skeletal RyRs. *Biophys. J.* 76:466*a* (Abstr.).

El-Hayek, R., B. Antoniu, J. Wang, S. L. Hamilton, and N. Ikemoto. 1995. Identification of calcium release-triggering and blocking regions of the II-III loop of the skeletal muscle dihydropyridine receptor. *J. Biol. Chem.* 270:22116–22118.

El-Hayek, R., and N. Ikemoto. 1998. Identification of the minimum essential region in the II-III loop of the dihydropyridine receptor α_1 subunit required for activation of skeletal muscle-type excitation-contraction coupling. *Biochemistry*. 37:7015–7020.

Jayaraman, T., A.-M. Brillantes, A. P. Timerman, S. Fleischer, H. Erdjument-Bromage, P. Tempst, and A. R. Marks. 1992. FK506 binding protein associated with the calcium release channel (ryanodine receptor). *J. Biol. Chem.* 267:9474–9477.

Lamb, G. D., and D. G. Stephenson. 1991. Effect of Mg^{++} on the control of Ca^{++} release in skeletal muscle fibres of the toad. *J. Physiol.* 434:507–528.

Lamb, G. D., and D. G. Stephenson. 1996. Effects of FK506 and rapamycin on excitation-contraction coupling in skeletal muscle fibres of the rat. *J. Physiol.* 494:569–576.

Laver, D. R., L. D. Roden, G. P. Ahern, K. R. Eager, P. R. Junankar, and A. F. Dulhunty. 1995. Cytoplasmic Ca^{2+} inhibits the ryanodine receptor from cardiac muscle. *J. Membr. Biol.* 147:7–22.

Laver, D. R., T. M. Baynes, and A. F. Dulhunty. 1997a. Magnesium inhibition of ryanodine receptor calcium channels: evidence for two independent mechanisms. *J. Membr. Biol.* 156:213–219.

Laver, D. R., V. J. Owen, P. R. Junankar, N. L. Taske, A. F. Dulhunty, and G. D. Lamb. 1997b. Reduced inhibitory effect of Mg^{2+} on ryanodine receptor Ca^{2+} release channels in malignant hyperthermia. *Biophys. J.* 73:1913–1924.

Leong, P., and D. H. Maclennan. 1998. A 37-amino acid sequence in the skeletal muscle ryanodine receptor interacts with the cytoplasmic loop between domains II and III in the skeletal muscle dihydropyridine receptor. *J. Biol. Chem.* 273:7791–7794.

Lu, X., L. Xu, and G. Meissner. 1994. Activation of the skeletal muscle calcium release channel by a cytoplasmic loop of the dihydropyridine receptor. *J. Biol. Chem.* 269:6511–6516.

Lu, X., L. Xu, and G. Meissner. 1995. Phosphorylation of dihydropyridine receptor II-III loop peptide regulates skeletal muscle calcium release channel function. *J. Biol. Chem.* 270:18459–18464.

MacKinnon, R., and C. Miller. 1988. Mechanism of charybdotoxin block of the high conductance Ca^{2+}-activated K^+ channel. *J. Gen. Physiol.* 91:335–349.

Marty, I., M. Robert, M. Villaz, K. S. De Jongh, Y. Lai, W. A. Catterall, and M. Ronjat. 1994. Biochemical evidence for a complex involving dihydropyridine receptor and ryanodine receptor in triad junctions of skeletal muscle. *Proc. Natl. Acad. Sci. USA*. 91:2270–2274.

Mayrleitner, M., A. P. Timerman, G. Wiederrecht, and S. Fleischer. 1994. The calcium release channel of sarcoplasmic reticulum is modulated by FK-506 binding protein: effect of FKBP-12 on single channel activity of the skeletal muscle ryanodine receptor. *Cell Calcium*. 15:99–108.

Mead, F. C., D. Sullivan, and A. J. Williams. 1998. Evidence for a negative charge in the conduction pathway of the cardiac ryanodine receptor channel provided by the interaction of K^+ channel N-type inactivation peptides. *J. Membr. Biol.* 163:225–234.

Melzer, W., E. Rios, and M. F. Schneider. 1987. A general procedure for determining the rate of calcium release from the sarcoplasmic reticulum in skeletal muscle fibers. *Biophys. J.* 51:849–863.

Minium, E. W., B. M. King, and G. Bear. 1993. Statistical Reasoning in Psychology and Education. John Wiley & Sons, Inc. Singapore. 484.

Murray, B. E., and K. Ohlendieck. 1998. Cross-linking analysis of the ryanodine receptor and α_1-dihydropyridine receptor in rabbit skeletal muscle triads. *Biochem. J.* 324:689–696.

Nakai, J., N. Sekiguchi, T. A. Rando, P. D. Allen, and K. G. Beam. 1998a. Two regions of the ryanodine receptor involved in coupling with L-type Ca^{2+} channels. *J. Biol. Chem.* 273:13403–13406.

Nakai, J., T. Tanabe, T. Konno, B. Adams, and K. G. Beam. 1998b. Localization in the II-III loop of the dihydropyridine receptor of a sequence critical for excitation-contraction coupling. *J. Biol. Chem.* 273:24983–24986.

Orlova, E. V., I. I. Serysheva, M. van Heel, S. L. Hamilton, and W. Chiu. 1996. Two structural configurations of the skeletal muscle calcium release channel. *Nat. Struct. Biol.* 3:547–551.

Radermacher, M., V. Rao, R. Grassucci, J. Frank, A. P. Timerman, S. Fleischer, and T. Wagenknecht. 1994. Cryo-electron microscopy and three-dimensional reconstruction of the calcium release channel/ryanodine receptor from skeletal muscle. *J. Cell Biol.* 127:411–423.

Sagara, Y., and G. Inesi. 1991. Inhibition of the sarcoplasmic reticulum Ca^{++} transport ATPase by thapsigargin at subnanomolar concentrations. *J. Biol. Chem.* 26612:13503–13506.

Saito, A., S. Seiler, A. Chu, and S. Fleischer. 1984. Preparation and morphology of sarcoplasmic reticulum terminal cisternae from rabbit skeletal muscle. *J. Cell Biol.* 99:875–885.

Tanabe, T., K. G. Beam, B. A. Adams, T. Niidome, and S. Numa. 1990. Regions of the skeletal muscle dihydropyridine receptor critical for excitation-contraction coupling. *Nature*. 346:567–568.

Timerman, A. P., E. Ogunbumni, E. Freund, G. Wiederrecht, A. R. Marks, and S. Fleischer. 1993. The calcium release channel of sarcoplasmic reticulum is modulated by FK-506-binding protein. *J. Biol. Chem.* 268:22992–22999.

Timerman, A. P., G. Wiederrecht, A. Marcy, and S. Fleischer. 1995. Characterization of an exchange reaction between soluble FKBP-12 and the FKBP-ryanodine receptor complex. *J. Biol. Chem.* 270:2451–2459.

Wagenknecht, T., R. Grassucci, J. Berkowitz, G. J. Wiederrecht, H.-B. Xin, and S. Fleischer. 1996. Cryoelectron microscopy resolves FK506-binding protein sites on the skeletal muscle ryanodine receptor. *Biophys. J.* 70:1709–1715.

Wagenknecht, T., M. Radermacher, R. Grassucci, J. Berkowitz, H. B. Xin, and S. Fleischer. 1997. Locations of calmodulin and FK506-binding protein on the three-dimensional architecture of the skeletal muscle ryanodine receptor. *J. Biol. Chem.* 272:32463–32471.

Wagenknecht, T., and M. Radermacher. 1997. Ryanodine receptors: structure and macromolecular interactions. *Curr. Opin. Struct. Biol.* 7:258–265.

Xu, L., G. Mann, and G. Meissner. 1996. Regulation of cardiac Ca^{2+} release channel (ryanodine receptor) by Ca^{2+}, H^+, Mg^{2+}, and adenine nucleotides under normal and simulated ischemic conditions. *Circ. Res.* 79:1100–1109.

Yamazawa, T., H. Takeshima, M. Shimuta, and M. Iino. 1997. A region of the ryanodine receptor critical for excitation-contraction coupling in skeletal muscle. *J. Biol. Chem.* 272:8161–8164.